International Symposium
On Turbulence and Shear Flow
Phenomena (TSFP-9)
June 30 - July 3, 2015 *Melbourne, Australia*

DRAG REDUCTION IN SPATIALLY DEVELOPING TURBULENT BOUNDARY LAYERS BY BLOWING AT CONSTANT MASS-FLUX

Yukinori Kametani
Linné FLOW Centre
KTH Mechanics
Osquars Backe 18, 100 44 Stockholm, Sweden
yukinori.kametani@mech.kth.se

Koji Fukagata
Department of Mechanical Engineering
Keio University
Hiyoshi 3-14-1, Yokohama 223-8522, Japan
fukagata@mech.keio.ac.jp

Ramis Örlü
Linné FLOW Centre
KTH Mechanics
Osquars Backe 18, 100 44 Stockholm, Sweden
ramis@mech.kth.se

Philipp Schlatter
Linné FLOW Centre
KTH Mechanics
Osquars Backe 18, 100 44 Stockholm, Sweden
pschlatt@mech.kth.se

Abstract

A series of large-eddy simulations of spatially developing turbulent boundary layers with uniform blowing at moderate Reynolds numbers (based on free-stream velocity, U_∞, and momentum thickness, θ) up to $Re_\theta \approx 2500$ were performed with the special focus on the effect of intermittent (separated in streamwise direction) blowing sections. The number of blowing sections, N, investigated is set to be 3, 6, 20, 30 and compared to $N = 1$, which constitutes the reference case, while the total wall-mass flux is constrained to be the same for all considered cases, corresponding to a blowing amplitude of 0.1% of U_∞ for the reference case. Results indicate that the reference case provides a net-energy saving rate of around 18%, which initially decreases at most 2 percentage points for $N = 3$ but recovers with increasing N. The initial reduction of the drag reduction is due to the shorter streamwise length of intermittent blowing sections. The physical decomposition of the skin friction drag through the FIK identity (Fukagata *et al.*, 2002), shows that the distribution of all components over each blowing section has similar trends, resulting in similar averaged values over the whole control region.

INTRODUCTION

The skin friction drag originating from fluid viscosity on surfaces of vehicles has a large economical and ecological impact from the viewpoint of fuel consumption. Due to the laminar-turbulent transition within boundary layers, the skin friction drag increases drastically compared to its laminar counterpart. In order to reduce the skin friction drag, but also to control other flow properties such as heat transfer, various passive and active flow control techniques have been devised. Typical examples of active control methods that have been examined are *e.g.* opposition control (Choi *et al.*, 1994), wall oscillations (Ricco & Quadrio, 2008) or wall deformations (Tomiyama & Fukagata, 2013). Most of these studies have been focused on internal flows, hence there is a need for investigations in external flows. Such studies are of practical importance, *e.g.* with respect to blowing and suction used for film-cooling on turbine blades and slotted wings, respectively.

One such investigation in a spatially developing turbulent boundary layer with uniform blowing and suction by means of direct numerical simulations (DNS), albeit at a low Reynolds number, is the work by Kametani & Fukagata (2011). They concluded that blowing achieves skin friction drag reduction, while suction stabilizes the turbulence in the boundary layer, and they quantitatively discussed different mechanism of those effects. In light of the recent advances in the understanding of the large/small-scale interaction (*cf.* Marusic *et al.*, 2010) and dominant flow structures (*cf.* Schlatter *et al.*, 2014), the effects of blowing and suction on the large-scale turbulent structures in high Reynolds number wall-turbulence is nearly unexplored. The recent developments in computational power enable numerical simulations at moderately high Reynolds numbers via DNS (Schlatter & Örlü, 2010). In particular, well-resolved large-eddy simulations (LES) have become a feasible alternative to DNS (and experiments) in order to reach even higher Reynolds numbers where a scale separation sets in and at the same time still provide data that are dynamically and kinematically of high quality (Eitel-Amor *et al.*, 2014). Kametani *et al.* (2014) performed a natural extension of the work by Kametani & Fukagata (2011) towards higher Reynolds numbers by means of well-resolved LES to both study the Reynolds number dependence as well as the influence of the control position and length. They concluded that the longer the streamwise length of the control region is the higher the control efficiency becomes. The studies of Kametani & Fukagata (2011) and Kametani *et al.* (2014) indicate, in particular, that a higher blowing amplitude results in larger drag reduction, and that a longer streamwise length of a uniform blowing region results in a larger drag reduction.

Recently, flow control by means of blowing is also experimentally studied and compared with results from numerical simulations (see *e.g.* Kornilov & Boiko, 2012). In this respect the question whether blowing should be applied over the full control domain or spatially intermittent has not

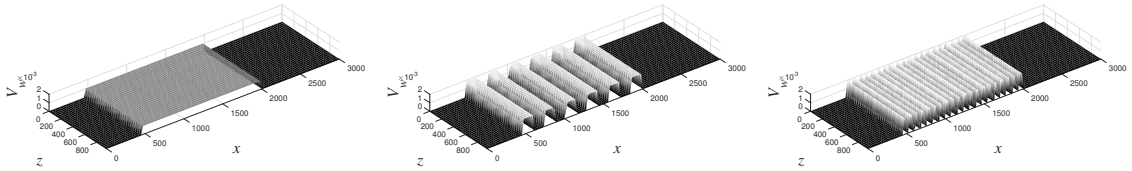

Figure 1. Distribution of the blowing velocity. *Left*, FULL; *center*, INT6; *right*, INT20.

been addressed yet, but is from practical relevance, since narrower blowing regions might be desirable from a maintenance and feasibility point of view.

In the present study, a series of large-eddy simulations of spatially developing turbulent boundary layers with uniform blowing at moderate Reynolds numbers (based on free-stream velocity, U_∞, and momentum thickness, θ) up to $Re_\theta \approx 2500$ were performed with the special focus on the effect of spatially intermittent, *i.e.* separated in streamwise direction, blowing sections. The dependency of the number of blowing sections on the overall effect of uniform blowing are examined with a constant total mass flux from the wall and fixed start and end locations of blowing, *i.e.* the blowing amplitude depends on the number of blowing section. Furthermore, the effects of the uniform blowing on the statistics with several numbers of blowing sections are investigated and the performance of drag reduction by blowing is discussed in terms of the net-energy saving rate. The FIK identity (Fukagata *et al.*, 2002) will as well be exploited to assess the effect of blowing on the physically decomposed components of the skin friction drag.

LARGE-EDDY SIMULATION

The governing equations are the incompressible continuity and Navier-Stokes equations. The ADM-RT model (Schlatter *et al.*, 2004) is used in the present large-eddy simulations. The momentum equations for the resolved velocity $\overline{u}_i$ and pressure $\overline{p}$ are written as

$$\frac{\partial \overline{u}_i}{\partial t} = -\overline{u}_j \frac{\partial \overline{u}_i}{\partial x_j} - \frac{\partial \overline{p}}{\partial x_i} + \frac{1}{Re} \frac{\partial^2 \overline{u}_i}{\partial x_j \partial x_j} - \chi H_N * \overline{u}_i \,. \qquad (1)$$

The values are non-dimensionalized by U_∞ and the inlet displacement thickness, δ_0^d. The corresponding Reynolds number is set to $Re = U_\infty \delta_0^d / \nu = 450$. The last term in the right-hand side of eq. (1) denotes the relaxation term, which is based on a higher-order three-dimensional filter operation where $H_N \equiv (I-G)^{N+1}$ is convoluted with $\overline{u}_i$, and G is a lower-order, low-pass filter. The computations have all been carried out in a domain $(L_x \times L_y \times L_z) = (3000 \times 100 \times 960)$ in streamwise, wall normal, and spanwise direction, respectively. The corresponding number of spectral collocation points is $(N_x \times N_y \times N_z) = (2048 \times 257 \times 1536)$. Due to the 3/2-rule for dealiasing in streamwise and spanwise directions, the maximum grid resolution in wall units is $(\Delta x^+ \times \Delta y^+_{max} \times \Delta z^+) = (20.9 \times 13.3 \times 8.9)$.

Uniform blowing is applied through an inhomogeneous wall-boundary condition for the normal velocity, $V_w = 1.0 \times 10^{-3}$ in the range of $800 < Re_{0,\theta} < 2100$, where the subscript 0 denotes the value from the uncontrolled case. The total mass flux from the wall is $M_0 = \int_S V_w \mathrm{d}S$. In order to investigate the spatial intermittency effect on uniform blowing, the full blowing section is separated into N-sections $(N = 1, 3, 6, 20, 30)$, referred to as FULL, INT3, INT6, INT20 and INT30, respectively. The corresponding blowing velocities are visualized in Fig. 1. As the number of sections N increases, the blowing area asymptotes to 50% of the FULL case and in turn the local maximum amplitude of blowing asymptotes to $V_w = 2.0 \times 10^{-3}$.

STATISTICS
FULL BLOWING

The effect of blowing on several statistics for the reference case is documented in Fig. 2. In this case, the blowing amplitude, V_w, is set to be 1.0×10^{-3}, *i.e.* 0.1% of U_∞. Note that for the present paper the statistics are scaled by wall units of the uncontrolled case, indicated through the superscript $+nc$, which enables a direct comparison of the effect on the turbulence statistics without bias introduced by the changed wall shear stress and hence friction velocity. This choice might also ease comparison with experimental investigations where the skin friction can often only be measured accurately in case of no control. As apparent from Fig. 2(a), the effect of blowing on the skin friction coefficient, c_f, is–as expected–significant. The gray line represents the correlation based on the $1/7^{\text{th}}$-power law, $c_f = 0.024 Re_\theta^{-1/4}$ (Smits *et al.*, 1983), and indicates that the boundary layer without control can be considered fully developed turbulent (*cf.* Schlatter & Örlü, 2012). The figure confirms that blowing reduces skin friction drag and that the boundary layer requires some relaxation time/distance to recover from the control and approach the uncontrolled skin friction relation.

The mean streamwise velocity profile in Fig. 2(b) shows that blowing effects the flow throughout the boundary layer height, *viz.* the mean velocity profile is pushed away from the wall. A similar effect can be evinced for the root-mean-square (RMS) of the streamwise (x), wall-normal (y) and spanwise (w) velocity fluctuations, Fig. 2(c), which show an increase of the turbulence level. In particular the outer layer appears to be more influenced by the control. The Reynolds shear stress (RSS) and the total shear stress (TSS), *i.e.* the summation of RSS and the viscous shear stress, are plotted in Fig. 2(d), and show that blowing enhances turbulence away from the wall. Note that in case the actual friction velocity of each flow case would have been used, the profiles for the blowing case would appear different (*cf.* Kametani *et al.*, 2014): the mean velocity profile would exceed the case with no blowing and the turbulence quantities would be further enhanced.

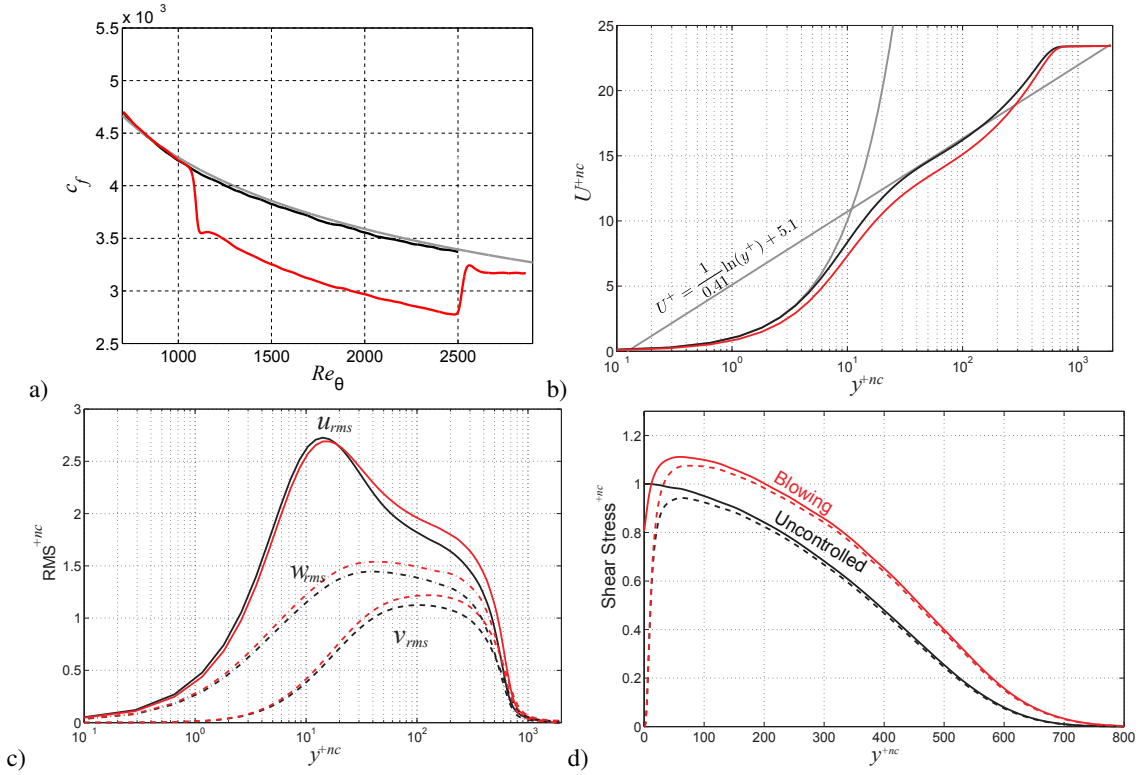

Figure 2. The statistics of the reference case (FULL) at $Re_{\theta,0} = 1800$. (a) skin friction coefficient, (b) streamwise mean velocity, (c) RMS profiles, and (d) Reynolds shear and total stresses. Black, uncontrolled; red, blowing; Grey: (a) correlation obtained from the $1/7^{\text{th}}$-power law, and (b) linear and logarithmic law.

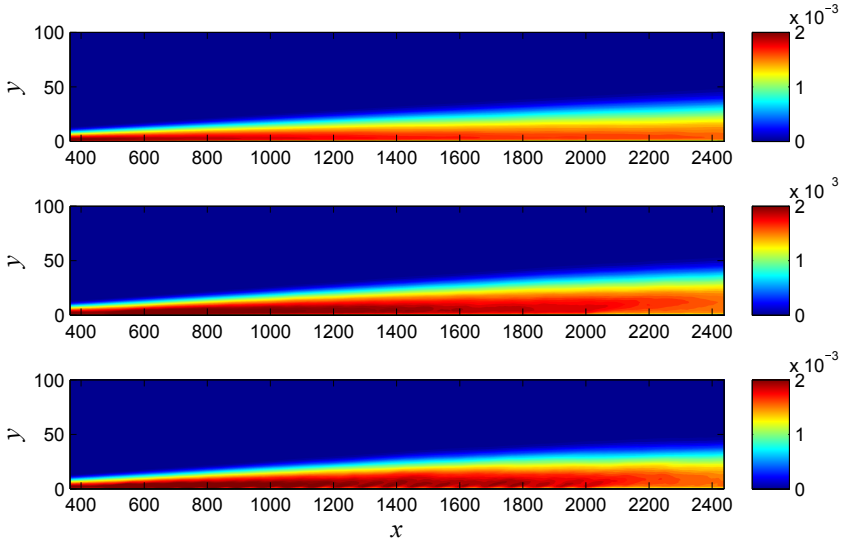

Figure 3. Reynolds shear stress scaled by free-stream velocity. *Top*, uncontrolled; *middle*, FULL; *bottom*, INT20. Note that the blowing region is $450 < x < 2000$.

INTERMITTENT BLOWING

To assess the effect of spatially intermittent blowing sections on the turbulence, figure 3 depicts the spatial development of the Reynolds shear stress distribution in the streamwise/wall-normal, *i.e.* $x-y$, plane. In order not to be biased by the changed boundary conditions at the wall, here the free-stream velocity is utilized for non-dimensionalisation. It is apparent that the Reynolds shear stress is enhanced over the blowing wall sections and the enhanced turbulence regions are convected downstream forming inclined distributions. Between the blowing walls, the enhancement of turbulence near the wall is interrupted.

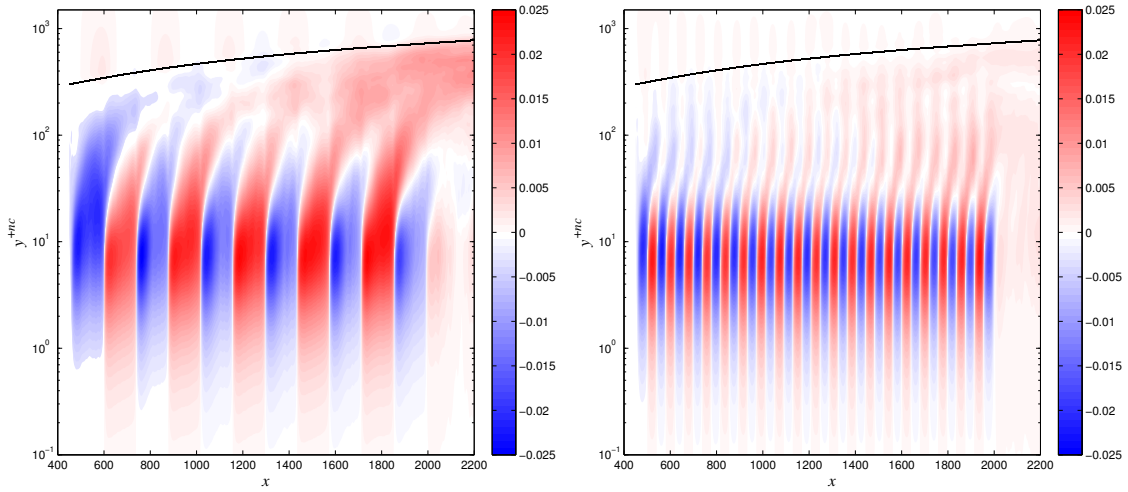

Figure 4. The difference between the mean streamwise velocity U of FULL case ($N = 1$) and intermittent cases, $\Delta U = U_{full} - U_{int}$ scaled with wall-units from the uncontrolled case. Left, $N = 6$; right, $N = 20$. Black solid line shows the 99% boundary layer thickness of the uncontrolled case.

In order to compare the mean streamwise velocity of the FULL and the intermittent blowing cases, the difference between the FULL and intermittent blowing cases, *viz.* $\Delta U = U_{full} - U_{int}$, scaled with wall units from the case without control, is shown in Fig. 4. On the blowing section of the intermittent blowing cases, the mean streamwise velocity is lower than that in the FULL case, while it is faster on the non-blowing region. Since the maximum blowing amplitude of the intermittent cases are higher than that of the FULL case, the amount of the shift of the mean streamwise velocity profile, U, into the wall-normal direction over the blowing wall is larger in the intermittent cases than in the FULL case. This results in a more moderate wall-normal gradient of the mean streamwise velocity, *viz.* $\frac{\partial U}{\partial y}$. On the other hands, in the non-blowing section, the velocity profiles show the opposite trend because of the absence of wall normal flux. Downstream the intermittent blowing region, the profile immediately begins to recover to that of the uncontrolled state, *i.e.* its profile shifts back to the wall. There is an increase of ΔU for $x > 1400$ and $y^{+nc} > 100$ that is visible for the INT6 case. This region seems to spread from the non-blowing region near the wall. Different from the FULL case, the turbulent boundary layer recovers intermittently from the non-blowing regions; an effect that weakens with increasing N.

FRICTION DRAG REDUCTION

The friction coefficient, c_f, is plotted in Fig. 5 against the Reynolds number of the uncontrolled case, corresponding to the same streamwise location. The plot shows that friction coefficient of the intermittent blowing case oscillates around the one of the FULL case. On the non-blowing region, the profile recovers immediately, which is not directly apparent when considering the skin friction at the same location; since the blowing cases correspond to a higher Reynolds number, *cf.* Fig. 2(a).

While blowing clearly achieves friction drag reduction, the control efficiency is important to assess in light of practical applications. The local drag reduction rate R^L and net-energy saving rate S^L can be defined as

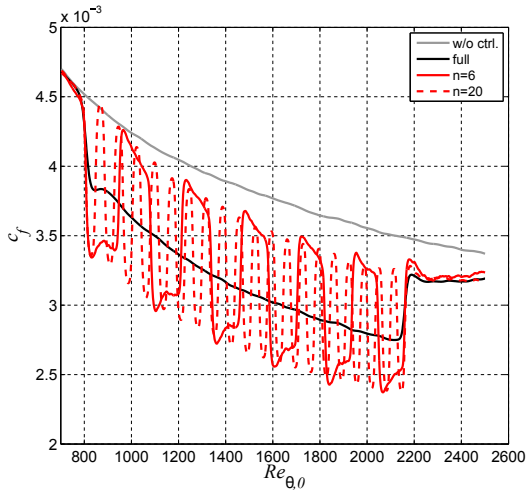

Figure 5. Skin friction coefficient, c_f, as function of Reynolds number based on the uncontrolled case.

$$R^L(x) = \frac{c_{f,0}(x) - c_f(x)}{c_{f,0}(x)}, \tag{2}$$

$$S^L(x) = \frac{c_{f,0}(x) - (c_f(x) + w_{in}(x))}{c_{f,0}(x)}, \tag{3}$$

respectively. Hereby, $w_{in}(x)$ denotes the control-input power defined as $0.5V_w^3$. Since in the present study, the blowing amplitude is quite small, *viz.* $V_w^3 = \mathcal{O}(10^{-9})$, the drag reduction rate and the net-energy saving rate is mostly equivalent. The mean net-energy saving rate, S,

$$S = \int_{x_s}^{x_e} \frac{c_{f,0}(x) - (c_f(x) + w_{in}(x))}{c_{f,0}(x)}\,\mathrm{d}x, \tag{4}$$

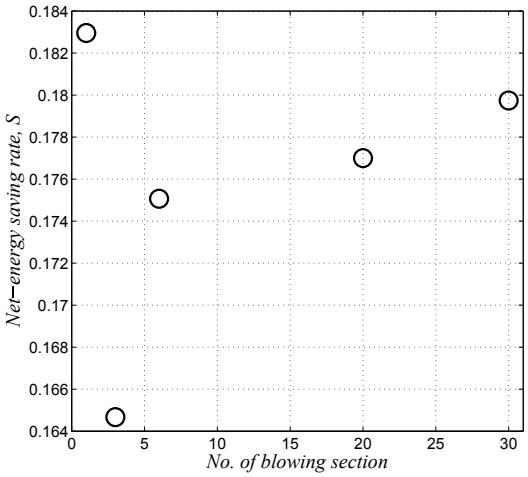

Figure 6. Net-energy saving rate as a function of the number of slots

where x_s and x_e denote the starting and ending location of the controlled region, is depicted as a function of the number of blowing sections N in Fig. 6. As apparent the reference case provides a net-energy saving rate of around 18%, which initially decreases at most 2 percentage points for $N = 3$ but recovers with increasing N. However, it rises up again and approaches that of the FULL case as N increases. Although the energy saving rate drops by 2 percent points at $N = 3$, the net-energy saving rate recovers with increasing N.

Decomposition of friction drag

The skin friction drag can be decomposed into different physical components by means of the FIK identity (Fukagata *et al.*, 2002), *viz.*

$$c_f(x) = c^{\delta}(x) + c^{T}(x) + c^{C}(x) + c^{D}(x) + c^{P}(x). \quad (5)$$

The terms on the right-hand side are the contributions from boundary layer thickness, Reynolds shear stress, wall-normal convection, spatial development and pressure gradient, respectively. For a more detailed discussion of each term see *e.g.* Kametani & Fukagata (2011). Similarly, the mean values are calculated by integration along the streamwise direction, *i.e.*

$$C_f = C^{\delta} + C^{T} + C^{C} + C^{D} + C^{P}. \quad (6)$$

Kametani & Fukagata (2011) concluded that the terms on the right hand sides, except the mean convection term C^C, in the uncontrolled case take positive values and the main contribution to the skin friction drag comes from the Reynolds shear stress and wall-normal convection. Figure 7 depicts the decomposed mean skin friction drag. The width of the bar denote the blowing region. It is apparent that the mean convection term takes negative values because the product of mean streamwise velocity and wall-normal velocity near the wall takes positive values, resulting in

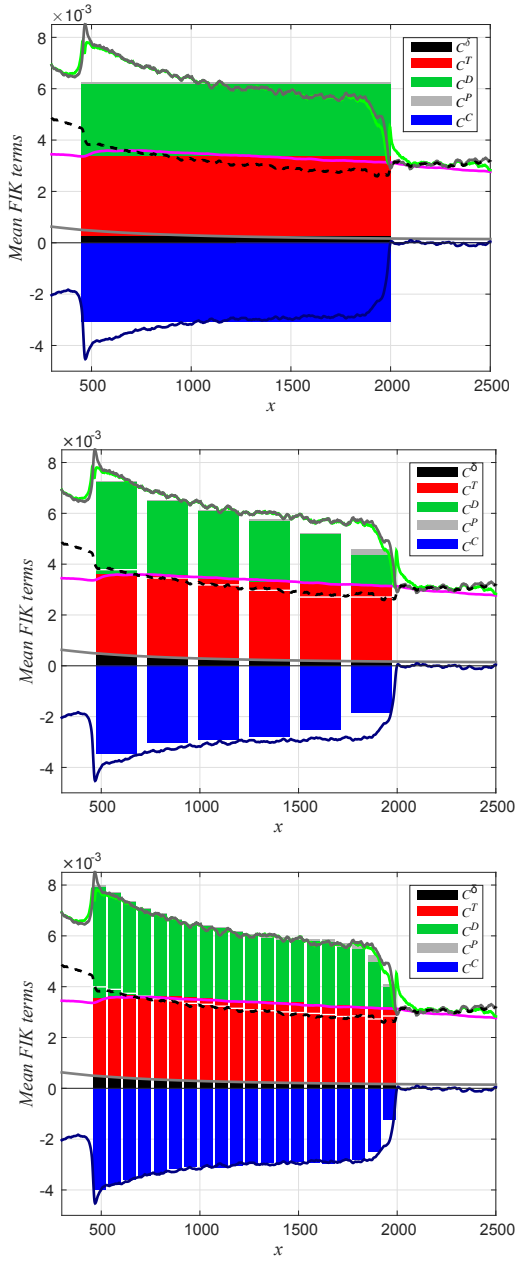

Figure 7. Streamwise averaged FIK terms. Top, FULL; middle, INT6; bottom, INT20. Lines are locally defined FIK identity of the FULL case.

the negative mean wall-normal convection term. Uniform blowing achieves the large drag reduction by enhancing the magnitude of the mean convection term. The FIK identity averaged over each blowing wall from the INT6 and INT20 cases are as well shown in Fig. 7. The line plot shows the local FIK identity of the FULL case defined by the FIK identity. Obviously the bar distribution asymptotes to the FULL case as the number of blowing section increases. Interestingly, the pressure gradient term is quite small above the whole blowing region in spite of the frequent starts and ends of the blowing. The created adverse and favourable pressure gradients by starting and stopping the blowing apparently cancel each other out.

It is notable that the local amplitude of the local maximum blowing amplitude asymptotes to twice that value of the FULL case. This fact indicates that the drag reduction effect of blowing depends on the total mass flux rather than the maximum blowing amplitude.

CONCLUSION

Large-eddy simulations of spatially developing turbulent boundary layers with streamwise intermittent uniform blowing sections with identical total mass flux from the wall were performed in order to investigate the effect of blowing on the drag reduction. The blowing region is separated into N sections, $N = 3$, 6, 20 and 30 and compared the reference case with $N = 1$. By separated blowing regions, the skin friction drag oscillates with immediate recovery on the non-blowing wall. For the reference case a net-energy saving rate of around 18% is achieved, which initially decreases at most 2 percentage points for $N = 3$ but recovers with increasing N. The drop of performance is, however, only 2 percent points compared to the fully uniform case. This fact indicates that the separated blowing wall still achieves large net-energy saving rates with the narrower blowing wall.

ACKNOWLEDGMENTS

This project is financially supported by the Japan Society for the Promotion of Science (JSPS). Computer time is provided by SNIC (Swedish National Infrastructure for Computing).

REFERENCES

Choi, H., Moin, P. & Kim, J. 1994 Active turbulent control for drag reduction in wall-bounded flows. *J. Fluid Mech.* **262**, 75–110.

Eitel-Amor, G., Örlü, R. & Schlatter, P. 2014 Simulation and validation of a spatially evolving turbulent boundary layer up to $Re_\theta = 8300$. *Int. J. Heat Fluid Flow* **47**, 57–69.

Fukagata, K., Iwamoto, K. & Kasagi, N. 2002 Contribution of Reynolds stress distribution to the skin friction in wall-bounded flows. *Phys. Fluids* **14**, L73–L76.

Kametani, Y. & Fukagata, K. 2011 Direct numerical simulation of spatially developing turbulent boundary layers with uniform blowing and suction. *J. Fluid Mech.* **681**, 154–172.

Kametani, Y., Örlü, Schlatter, P. & Fukagata, K. 2014 Drag reduction in turbulent boundary layers: effect of uniform blowing and suction. In *Proceedings of 10th International ERCOFTAC Symposium on Engineering Turbulence Modelling and Measurement*. Marbella, Spain.

Kornilov, V. & Boiko, A. 2012 Efficiency of air microblowing through mictoperforated wall for flat plate drag reduction. *AIAA J.* **50**, 724–732.

Marusic, I., Mathis, R. & Hutchins, N. 2010 Predictive model for wall-bounded turbulent flow. *Science* **329**, 193–196.

Ricco, P. & Quadrio, M. 2008 Wall-oscillation conditions for drag reduction in turbulent channel flow. *Int. J. Heat Fluid Flow* **29**, 601–612.

Schlatter, P., Li, Q., Örlü, R., Hussain, F & Henningson, D. S. 2014 On the near-wall vortical structures at moderate Reynolds numbers. *Eur. J. Mech. B-Fluid* **48**, 75–93.

Schlatter, P. & Örlü, R. 2010 Assessment of direct numerical simulation data of turbulent boundary layers. *J. Fluid Mech.* **659**, 116–126.

Schlatter, P. & Örlü, R. 2012 Turbulent boundary layers at moderate Reynolds numbers: inflow length and tripping effects. *J. Fluid Mech.* **710**, 5–34.

Schlatter, P., Stolz, S. & Kleiser, L. 2004 Les of transitional flows using approximate deconvolution model. *Int. J. Heat Fluid Flow* **25-3**, 549–558.

Smits, A. J., Matheson, N & Joubert, P N 1983 Low-Reynolds-number turbulent boundary layers in zero and favorable pressure gradients. *J. Ship Res.* **27**, 147–157.

Tomiyama, N. & Fukagata, K. 2013 Contribution of Reynolds stress distribution to the skin friction in wall-bounded flows. *Phys. Fluids* **25**, 105115.